AN ATLAS OF PHOTOSPHERIC MAGNETIC FIELD OBSERVATIONS AND COMPUTED CORONAL MAGNETIC FIELDS: 1976–1985

J. TODD HOEKSEMA and PHILIP H. SCHERRER

Center for Space Science and Astrophysics, Stanford University, Stanford, CA 94305, U.S.A.

(Received 18 March, 1986)

Abstract. Daily magnetogram observations of the large-scale photospheric magnetic field have been made at the John M. Wilcox Solar Observatory at Stanford since May of 1976. These measurements provide a homogeneous record of the changing solar field through most of solar cycle 21.

Using the photospheric data, the configuration of the coronal and heliospheric fields can be calculated using a Potential Field – Source Surface model. This provides a three-dimensional picture of the heliospheric field evolution during the solar cycle.

In this note we announce the publication of UAG Report No. 94, an Atlas containing the complete set of synoptic charts of the measured photospheric magnetic field, the computed field at the source surface, and the coefficients of the multipole expansion of the coronal field. The general underlying structures of the solar and heliospheric fields, which determine the environment for solar–terrestrial relations and provide the context within which solar activity related events occur, can be approximated from these data.

1. Introduction

The large-scale magnetic field of the Sun evolves slowly but dramatically during the 11 years of a sunspot cycle. Because the changes occur relatively slowly, much can be learned about the ambient environment within which activity related events occur by studying the large scale field configuration over longer periods of time.

Full disk measurements of the mean solar magnetic field began at Stanford in 1975. Observations of the photospheric field with a resolution of three arc minutes began in May 1976 and have continued through the present time. Synoptic charts of the photospheric field have been published monthly in the Prompt Reports of *Solar Geophysical Data* beginning with the data from January, 1979.

Since the data now span most of a sunspot cycle, beginning with solar minimum in 1976, continuing through maximum in 1979, and covering much of the declining phase through mid 1985, this was an appropriate time to publish all the data in one report for easy reference.

One important use of this data is in determining the configuration of the interplanetary magnetic field (IMF) by means of a Potential Field–Source Surface model. With this model, described by Hoeksema *et al.* (1982, 1983) and Hoeksema (1984), the three-dimensional polarity structure of the interplanetary medium can be calculated from the photospheric field measurements. Comparison with IMF measurements and coronameter data suggests a good level of agreement with the actual coronal and interplanetary field configurations (e.g., Wilcox and Hundhausen, 1983; Hoeksema, 1984; and Bruno

Solar Physics **105** (1986) 205–211.

et al., 1984). Synoptic charts of the heliospheric field configuration are also presented in the Atlas.

Finally, one intermediate result in the potential field calculation is a description of the coronal field in terms of its multipole components: dipole, quadrupole, etc. From these components the three-dimensional field near the Sun can be calculated. The relative contributions of the multipoles to the total field vary with height above the photosphere and with time during the solar cycle. Because the field is constantly changing, the values of the components are presented for each 180° of Carrington longitude.

Short descriptions of the observing instrument, the method of observation, data reduction, and model computation are provided here and in the Atlas. More detailed descriptions may be found in the referenced reports.

2. The Photospheric Field

Daily magnetograms with three arc min resolution are taken at the John M. Wilcox Solar Observatory at Stanford every day that the weather is good. A Babcock solar magnetograph measures the line-of-sight component of the photospheric magnetic field using the Zeeman splitting of the 5250.2 Å Fe I spectral line. This method accurately measures large-scale, weak field regions, but only crudely shows regions of strong or complex fields. The noise level of each measurement is less than 10 μT and the zero level error is less than 5 μT (1 G is 100 μT). Because of the saturation of the magnetic signal in the magnetograph, the measured values are smaller than the actual field strengths by about a factor of 2. A detailed description of the instrument can be found in Scherrer *et al.* (1977), Duvall (1977), or Hoeksema (1984).

The daily magnetograms are interpolated onto a finer grid based on the Carrington coordinate system. These maps are assembled into synoptic charts with each field measurement weighted by the central meridian distance and the quality of the measurement to provide the best determination of the solar field. Because of the large aperture size, the regions from 70° to the poles lie entirely within the last aperture and are not resolved.

Figure 1, an example from 1981, shows a contour map of the photospheric field from Carrington rotation 1713. The contour levels have the values indicated. Positive contours are solid, negative are dashed, and the zero line is heavy solid. The Atlas is shaded gray to aid the eye in recognizing patterns of strong and weak field regions. The gray scale is white at zero field values and saturates at the highest field value for the particular map. The shading is the same for positive and negative fields of equal magnitude. Gray shaded contour maps of the solar field are presented in the Atlas for Carrington rotations 1641 through 1766, from May 1976 through September 1985.

The Carrington coordinate system specifies the central meridian longitude, thus time goes from right to left on the Carrington grid simulating the rotation of the Sun. The dates of central meridian passage are labeled. The scale is the standard 8 mm day^{-1}. The inverted carets indicate the times of magnetograms contributing to the field data.

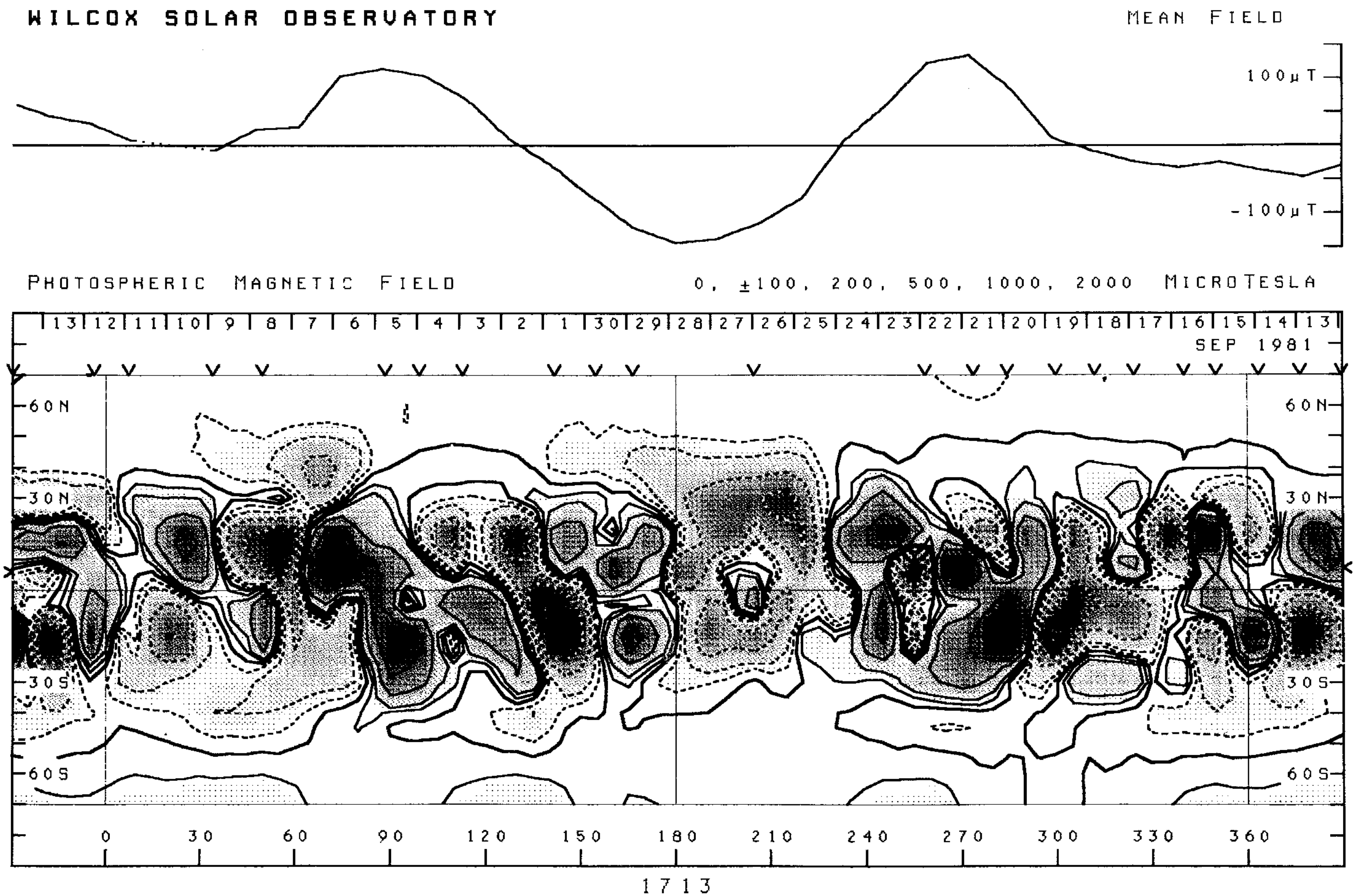

Fig. 1. A gray-level contour map showing the line-of-sight photospheric magnetic field for Carrington rotation 1713. Contour lines are at the values indicated. Negative contours are dashed. The heavy line denotes the zero field level. Gray shading intensifies with increasing field magnitude and is the same for positive and negative field regions. Independent measurements of the mean magnetic field of the Sun are shown in the upper panel.

An extra 30° are shown at each end of the rotation for continuity. Note that opposite ends of a rotation are not the same because of field evolution and differential rotation.

The top panel of the chart shows the mean magnetic field of the Sun as measured in integrated sunlight for each day. This is the result of a separate observation taken at the solar observatory. Dotted lines are linear interpolations over missing days.

3. The Heliospheric Field

Under the assumptions that the coronal field is approximately a potential field and that the field at some height above the photosphere is completely radial, as suggested by eclipse pictures and energy density considerations, the field configuration can be calculated from the photospheric measurements. While some changes in the field configuration probably occur above the radius where the field lines are assumed to become radial, called the source surface radius, we assume that the polarity structure is essentially locked in at that point and advected radially outward by the solar wind into the heliosphere. These are simplifying assumptions and although each of these assumptions is not strictly true, the overall picture which emerges conforms quite well to the available data.

This model was first developed independently by Schatten *et al.* (1969) and by Altschuler and Newkirk (1969). Later investigations (e.g., Adams and Pneuman, 1976; Altschuler *et al.*, 1976; Schultz *et al.*, 1978; Levine, 1982; Hoeksema, 1984; and references therein) demonstrated the basic validity of the model for predicting the large scale structure and suggested improvements for looking at the finer scale. The results presented in this report are extensions of the calculations of Hoeksema *et al.* (1982, 1983) and Hoeksema (1984). The source surface radius has been located at 2.5 solar radii because it gives the best overall agreement with the polarity pattern observed at Earth.

As described in Hoeksema *et al.* (1982, 1983) and Hoeksema (1984), three corrections have been applied to the data: elimination of the zero offset, or monopole component; addition of a strong polar field; and reconstruction of missing data in the synoptic charts.

A gray shaded contour map of the source surface magnetic field is shown in Figure 2. The layout is the same as for the photospheric field, with the grid once again showing slightly more than one Carrington rotation. The broad neutral line divides the negative polarity regions, shown by dashed contours, from the positive areas, indicated by solid lines. Notice that the field strength is about 1% that found at the photosphere. Maps of the source surface magnetic field are also presented in the Atlas for Carrington rotations 1641 through 1766.

Since we assume this field is carried radially outward by the motion of the solar wind, these graphs show the predicted three dimensional structure of the heliospheric field. It should be pointed out that much beyond 1 AU the interaction of various streams with even slightly different velocities will distort this structure (Suess and Hildner, 1985). The solar latitude of the Earth is shown by the small '>' and '<' symbols at the edges of each

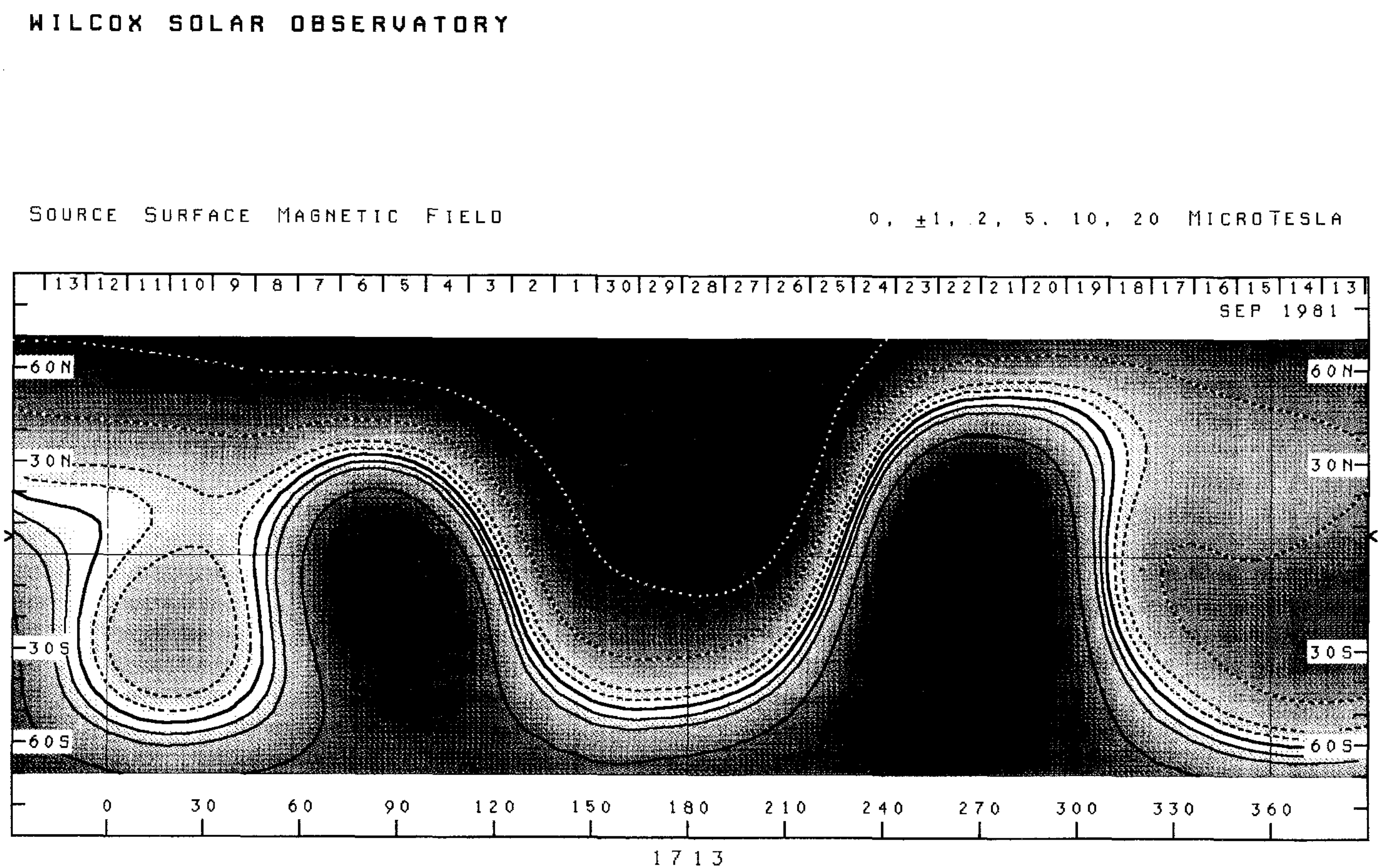

Fig. 2. A similar map of the radial field computed at the source surface also for Carrington rotation 1713. Note that the field values are much lower than at the photosphere and that the field structures are much simpler.

graph. To compare with the IMF polarity observed at Earth the travel time of the solar wind must be taken into account. Near the neutral line the transit time is typically 4.5 to 5 days. Thus to find the field extrapolated to Earth, look 60 to 65° west (i.e., right) of the desired date's central meridian longitude.

4. The Multiple Components

The mathematical solution can be summarized as follows: using the observed line-of-sight photospheric field as one boundary condition and the requirement of a purely radial field at the source surface as the other, a solution is found to LaPlace's equation (the potential field assumption) in terms of the Legendre polynomials.

The coefficients of the Legendre polynomials specify the relative magnitudes of the multipole components of the field near the Sun and can be used to reconstruct the large scale field in the low corona. This computation has been carried out several times for each Carrington rotation to minimize the effects of field evolution. Since the solar field evolves slowly, tables of the coefficients for the multipole components of the global field are provided each half Carrington rotation (approximately twice per month).

It is interesting to note that the heliospheric field is often characterized in terms of its lowest order components, particularly the dipole term. Near minimum the polar dipole is the dominant term, but during much of the solar cycle the quadrupole and octupole components contribute a comparable fraction of the field strength. This suggests that during much of the cycle the notion of a dipole or tilted dipole field is too simple and the importance of the higher order terms must be acknowledged (Hoeksema and Scherrer, 1984).

5. Conclusions

It is our hope that the provision of a homogeneous dataset of the solar magnetic field over nearly an entire sunspot cycle in a convenient, inclusive package will stimulate the studies of the large-scale structures of the solar and heliospheric magnetic field, encourage others to consider the relationship of the large-scale, ambient field structures to activity on short time scales and smaller spatial scales, and enable the inclusion of the heliospheric field in analyses of solar-terrestrial relations.

It is our intention to promote the use of these synoptic observations as primary data and for use in correlative studies in solar physics and solar-terrestrial physics research. We ask only that the source of the data be acknowledged and that we receive a copy of resulting research reports and papers. Copies of the Atlas are available upon request. Inquiries concerning the Atlas should be directed to: J. Todd Hoeksema or Philip H. Scherrer, Center for Space Science and Astrophysics, Stanford University, ERL 328, Stanford, CA 94305.

Acknowledgements

The existence of this data and the John M. Wilcox Solar Observatory would not have been possible without the foresight and persistence of John M. Wilcox.

Without long term funding such records can not be compiled. Over the years this work has been faithfully supported by the Office of Naval Research under Contracts N00014–76–C–0207 and N0014–86–K–0085, by the National Aeronautics and Space Administration under Grant NGR05–020–559 and Contract NAS5–24420, by the Atmospheric Sciences Section of the National Science Foundation under Grants ATM74–19007, ATM77–20580, ATM80–20421, ATM83–13271 and by the Max C. Fleischman Foundation.

We would also like to thank the observers: E. Gustavson, S. Bryan, J. T. Hoeksema, P. Duffy, J. Foster III, and H. Henning; and J. Alderman and H. Coffey for their assistance.

References

Adams, J. and Pneuman, G. W.: 1976, *Solar Phys.* **46**, 185.

Altschuler, M. D., Levine, R. H., Stix, M., and Harvey, J. W.: 1976, *Solar Phys.* **51**, 345.

Altschuler, M. D. and Newkirk, G. Jr.: 1969, *Solar Phys.* **9**, 131.

Bruno, R., L. F. Burlaga, L. F., and Hundhausen, A. J.: 1984, *J. Geophys. Res.* **89**, 5381.

Duvall, T. L., Jr.: 1977, Ph. D. Thesis, SUIPR Report No. 724.

Hoeksema, J. T.: 1984, Ph. D. Thesis, CSSA Report No. 7.

Hoeksema, J. T. and Scherrer, P. H.: 1986, *Report VAG-94*, Publ. U.S. Dept. of Commerce, Boulder, Colo., U.S.A.

Hoeksema, J. T. and Scherrer, P. H.: 1984, in *The Hydromagnetics of the Sun*, Proceedings of the Fourth European Meeting on Solar Physics, ESA SP-220, pp. 269.

Hoeksema, J. T., Wilcox, J. M., and Scherrer, P. H.: 1982, *J. Geophys. Res.* **87**, 10331.

Hoeksema, J. T., Wilcox, J. M., and Scherrer, P. H.: 1983, *J. Geophys. Res.* **88**, 9910.

Levine, R. H.: 1982, *Solar Phys.* **79**, 203.

Schatten, K. H., Wilcox, J. M., and Ness, N. F.: 1969, *Solar Phys.* **6**, 442.

Scherrer, P. H., Wilcox, J. M., Svalgaard, L., Duvall, T. L., Jr., Dittmer, P. H., and Gustafson, E. K.: 1977, *Solar Phys.* **54**, 353.

Schultz, M., Frazier, E. N., and Boucher, D. J., Jr.: 1978, *Solar Phys.* **60**, 83.

Solar Geophysical Data, Publ. U.S. Dept. of Commerce, Boulder, Colorado, U.S.A., 80302.

Suess, S. T. and Hildner, E.: 1985, *J. Geophys. Res.*, **90**, 9461.

Wilcox, J. M. and Hundhausen, A. L.: 1983, *J. Geophys. Res.* **88**, 8095.